Astronomy & Astrophysics

LETTER TO THE EDITOR

Detection of CO in Triton's atmosphere and the nature of surface-atmosphere interactions[*]

E. Lellouch[1], C. de Bergh[1], B. Sicardy[1,2,**], S. Ferron[3], and H.-U. Käufl[4]

[1] LESIA, Observatoire de Paris, 5 place Jules Janssen, 92195 Meudon, France
e-mail: emmanuel.lellouch@obspm.fr
[2] Université Pierre et Marie Curie, 4 place Jussieu, 75005 Paris, France
[3] ACRI-ST, 260 route du Pin Montard, BP 234, 06904 Sophia-Antipolis Cedex, France
[4] European Space Observatory, Karl-Schwarzschild-Strasse 2, 85748 Garching bei München, Germany

ABSTRACT

Context. Triton possesses a thin atmosphere, primarily composed of nitrogen, sustained by the sublimation of surface ices.
Aims. We aim at determining the composition of Triton's atmosphere to constrain the nature of surface-atmosphere interactions.
Methods. We perform high-resolution spectroscopic observations in the 2.32–2.37 μm range, using CRIRES at the VLT.
Results. From this first spectroscopic detection of Triton's atmosphere in the infrared, we report (i) the first observation of gaseous methane since its discovery in the ultraviolet by Voyager in 1989; and (ii) the first ever detection of gaseous CO in the satellite. The CO atmospheric abundance is remarkably similar to its surface abundance, and appears to be controlled by a thin, CO-enriched, surface veneer resulting from seasonal transport and/or atmospheric escape. The CH_4 partial pressure is several times higher than inferred by Voyager. This confirms that Triton's atmosphere is seasonally variable and is best interpreted by the warming of CH_4-rich icy grains as Triton passed southern summer solstice in 2000. The presence of CO in Triton's atmosphere also affects its temperature, photochemistry, and ionospheric composition. An improved upper limit on CO in Pluto's atmosphere is also reported.

Key words. planets and satellites: atmospheres – Kuiper belt: general

1. Introduction

Like Pluto, Neptune's satellite and probably former Kuiper-Belt object Triton possesses a tenuous, predominantly nitrogen atmosphere, in equilibrium with surface ices mostly composed of N_2 and a variety of other species. The most volatile of these species, CH_4 and CO, must be present in trace amounts in the atmosphere as well. However, depending on the precise mechanisms of surface-atmosphere interactions, the expected atmospheric abundances vary by orders of magnitude, and except for the detection of CH_4 in the UV by Voyager in 1989, observations have been severely lacking. Progress in IR-detector technology has now made the remote study of thin and distant atmospheres possible. Following our observations of methane in Pluto's atmosphere (Lellouch et al. 2009), we report the first spectroscopic detection of Triton's atmosphere in the infrared.

2. VLT/CRIRES observations and CH₄ and CO measurements

Spectroscopic observations of Triton were obtained on July 4, 2009, using the CRIRES infrared echelle spectrograph (Käufl et al. 2004) installed on ESO VLT (European Southern Observatory Very Large Telescope) UT1 (Antu) 8.2 m telescope. We focused on the regions of the (2–0) band of carbon monoxide and the $\nu_3+\nu_4$ band of methane, covering the 2318–2330, 2334–2345, 2349–2359, and 2363–2373 nm ranges. We used the instrument in adaptive optics mode with a slit of 0.4″, providing
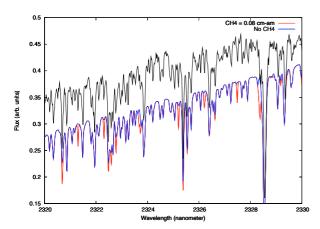
a mean spectral resolution of 60 000, and acquired spectra during ~4 h. A large Doppler shift (–23 km s⁻¹) ensured proper separation of the target lines from the telluric absorptions.

The resulting spectrum shows the detection of many lines due to methane in Triton's atmosphere, particularly at 2320–2330 nm (Fig. 1). This is the first observation of gaseous methane since its discovery by Voyager (Herbert & Sandel 1991). As for our study of Pluto's CH_4, we constructed a direct line-by-line atmospheric model of Triton, integrated over angles and including solar lines reflected off Triton's surface as well as the telluric transmission (see details in Lellouch et al. 2009). The spectrum was first modelled by assuming a single-temperature layer, with Triton's atmospheric methane mean temperature (T) and column density (a) as free parameters. We inferred $T = 50^{+20}_{-15}$ K and $a = 0.08 \pm 0.03$ cm-am (Fig. 2 online). The same analysis for Pluto inferred $T = 90^{+25}_{-18}$ K and $a = 0.75^{+0.55}_{-0.30}$ cm-am. This confirms that Pluto's atmosphere is warmer than Triton's, as a result of its higher methane abundance.

The error bars in the inferred mean methane temperature are too large to constrain the methane vertical distribution. Instead, we used the Voyager-determined thermal structure (temperature versus altitude, Krasnopolsky et al. 1993) and methane vertical profile (Herbert & Sandel 1991, ingress UV occultation profile). The latter shows a decrease in the CH_4 mixing ratio with altitude with a scale height of ~20 km, due to photolysis. We obtained the same column density as above, indicating a partial pressure of methane of 9.8 ± 3.7 nbar, i.e., a surface density of $(1.9 \pm 0.7) \times 10^{12}$ cm⁻³. This appears to be $4^{+5}_{-2.5}$ times higher than inferred from Voyager in 1989, adopting the CH_4 number densities of Herbert & Sandel (1991) and Strobel & Summers (1997)
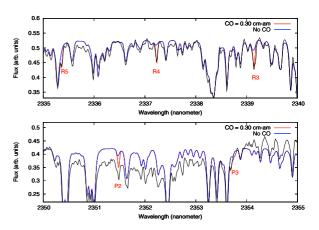
Fig. 1. Black: Triton spectrum at 2320–2330 nm observed by CRIRES/VLT. The spectral resolution is 60 000. Red and blue curves show synthetic spectra, including telluric and solar lines. Red: methane column density in Triton's atmosphere = 0.08 cm–am. Triton's thermal profile, based on Voyager measurements, is taken from Krasnopolsky (1993) and a Voyager-like vertical distribution is used for methane (Herbert & Sandel 1991, entrance profile). Blue: no methane. The continuum slope is caused by the red wing of the $\nu_3 + \nu_4$ band of solid methane. Here, as in Fig.3, the vertical unit approximately represents the geometric albedo (but uncorrected for telluric and solar lines). Models are shifted vertically by –0.07 for clarity.

$(4.7 \times 10^{11}$ cm^{-2} within a factor of 1.7, averaging ingress and egress). An even greater enhancement factor (5^{+6}_{-2}) is found if the Krasnopolsky & Cruikshank (1995) reanalysis of the Voyager UV data, which gives CH$_4$ = $3.1 \pm 0.8 \times 10^{11}$ cm^{-3} at the surface, is used. Results are independent of the surface pressure, as collisional broadening is negligible. They clearly demonstrate that the CH$_4$ partial pressure has increased in the past 20 years.

The 2335–2365 nm part of the Triton spectrum (see excerpts in Fig. 3) shows the detection of 8 lines due to the CO(2–0) band (R2-R5, P2, P3, P5 and P8), providing the first detection of CO in its atmosphere. An accurate determination of the CO abundance is difficult, because at infinite spectral resolution, these features are very narrow, saturated Doppler-shaped lines. Nonetheless, assuming a vertically uniform CO distribution, and utilizing the whole set of CO lines (see Fig. 4 online), we determine a CO column of 0.30 cm-am, i.e., a CO partial pressure of 24 nbar, within a factor of 3. The column density CO/CH$_4$ ratio is nominally ~3.75 (surface partial pressure ratio CO/CH$_4$ ~2.5) with a factor of 4 uncertainty. Deriving the CO/N$_2$ and CH$_4$/N$_2$ mixing ratio is complicated by the surface pressure in 2009 being unknown. Stellar occultation results (Olkin et al. 2007; Sicardy et al. 2003; Elliot et al. 1998, 2000a) indicate that the pressure has doubled in ~10 years from the 14 μbar value determined by Voyager in 1989 (Gurrola 1998). A reasonable assumption for 2009 is 40 μbar, which provides CO/N$_2$ ~ 6×10^{-4} and CH$_4$/N$_2$ ~ 2.4×10^{-4} at the surface, to within factors of 3 and 1.4, respectively. The CO abundance that we determine is many times lower than previous upper limits (Broadfoot et al. 1989; Young et al. 2001).

3. Discussion

Near-infrared observations have detected CO and CH$_4$ on Triton's surface with mixing ratios of 0.05% and 0.1% relative to N$_2$, and, at least for CH$_4$, mostly in solid solution in N$_2$ (Cruikshank et al. 1993; Quirico et al. 1999; Grundy et al. 2010). In this situation, the expected partial pressure of each species is the product of its solid mole fraction and its pure vapor pressure (Raoult's law for an ideal mixture). This scenario

Fig. 3. Black: portions of the Triton spectrum at 2335–2340 nm and 2350–2355 nm. Five CO lines (R5, R4, R3, P2 and P3) are present in these spectral ranges. Red and blue curves show synthetic spectra, including telluric and solar lines, as well as Triton's methane. Red: CO column density in Triton's atmosphere = 0.30 cm-am. Blue: No CO. The mismatch in the "continuum" level over 2351–2354 nm is caused by absorption in the (2–0) band of CO ice (see e.g. Quirico et al. 1999; Grundy et al. 2010), not included in models.

implies atmospheric abundances of CO and CH$_4$ about 1 and 3 orders of magnitude lower than observed, respectively (Fig. 5). Although Henry's law may be more applicable to the N$_2$-CH$_4$ system than Raoult's, this does not reduce the discrepancy by more than a factor of 2–3. This problem has been studied in the case of Pluto's atmospheric methane, present at the 0.5% level (Young et al. 1997; Lellouch et al. 2009), i.e. also considerably enriched over its solid solution equilibrium value. The origin of this enhancement is thought to ultimately lie in the seasonal evolution of the N$_2$-dominated solid solution. Preferential sublimation of N$_2$ initially creates a thin surface layer enriched in the less volatile species. Further evolution of this layer may lead to either (i) the formation of chemically pure grains in vertically or geographically segregated deposits ("pure ice" scenario); or (ii) the establishment of a homogeneous "detailed balancing layer" controlling the surface-atmosphere exchanges. In the "pure ice" case, the atmospheric mixing ratios are in simple proportion of the pure vapor pressures at the relevant ice temperatures (which may differ for different species) and, except for the main species controlling the pressure, of the fractional area covered by each ice. For CH$_4$ on Pluto, Stansberry et al. (1996) demonstrated that pure CH$_4$ lag deposits (whose existence has been proven by observations, see Douté et al. 1999) assume higher temperatures than N$_2$ because of their reduced sublimation cooling and preferential formation in regions of high insolation. Even if covering only a few percent of Pluto's surface, these patches can explain the observed atmospheric abundance of methane. Alternatively, the "detailed balanced" model (Trafton 1990; Trafton et al. 1998) predicts that surface-atmosphere exchanges in the presence of atmospheric escape and seasonal transport lead to an atmospheric composition reflecting that of the accessible ice reservoir from which it is replenished. When no fractionation (e.g., diffusive) occurs during escape or transport, the atmospheric mixing ratios are identical to those in the volatile reservoir. This is accomplished by the thin surface veneer, enriched in the less volatile species, throttling off the N$_2$ sublimation, and in permanent equilibrium with the atmosphere according to Raoult's law.

Our observations provide discriminating keys between these scenarios. The case for CO is most straightforward because: (i) CO is not subject to diffusive separation from N$_2$ upon
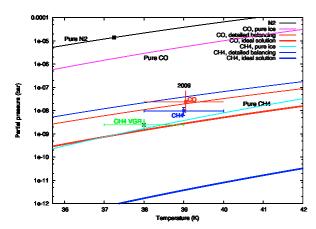
Fig. 5. Abundance measurements and equilibrium curves for Triton's volatiles. The black, pink, and light blue curves show the vapor pressure of pure N_2, CO, and CH_4 ices, calculated from Fray and Schmitt (2010). For CO and CH_4, the thick curves (red and blue, respectively) show the partial pressures based on Raoult's law for an ideal solid solution with N_2, with CO and CH_4 respective abundances of 5×10^{-4} and 1×10^{-3} in the ice (Quirico et al. 1999). For CO and CH_4, the thin red and blue lines show the partial pressures expected in the framework of the "detailed balancing model" (see text). The black square shows the 1989 Voyager pressure measurement (14 nbar), which corresponds to sublimation equilibrium of N_2 ice at 37.25 K. The green symbol represents the Voyager-measured CH_4 partial pressure (Herbert & Sandel 1991); it is plotted at 38 ± 1 K, the surface temperature measured by Voyager and the N_2 ice temperature inferred by Tryka et al. (1994). The blue star and the red square show the CH_4 and CO abundances determined in this work. They are plotted at a temperature of 39 ± 1 K. A temperature of 39 K corresponds to a plausible 40 μbar pressure for Triton's atmosphere in 2009; 40 K, which corresponds to a N_2 vapor pressure of 65 μbar, is a reasonable upper limit, given the stellar occultation inferences that Triton's surface pressure has doubled in the 10 years following the Voyager epoch. The CO partial pressure we measure is consistent with expectations from the detailed balancing model, while CH_4 is lower.

escape; and (ii) as the ratio of its vapor pressure to that of N_2 is largely insensitive to temperature in the relevant range (e.g., CO/N_2 = 0.112 at 36 K and 0.166 at 41 K), its atmospheric mixing ratio should be roughly seasonally constant. The observed CO abundance is over two orders of magnitude lower than the pure CO vapor pressure (Fig. 5), and one might envisage that the atmospheric CO results from the sublimation of pure CO patches covering ~0.4% of the surface. However, we regard this scenario as unlikely. Although the pure vs. isolated form of CO on Triton's surface has not been proven by observations, the miscibility of CO and N_2 in the solid phase in all proportions and the similarity of their vapor pressures argue for a co-condensation of the two species on Triton's surface. This is further supported by the remarkably similar longitudinal distribution of the N_2 and CO ice bands at Triton (Grundy et al. 2010), strongly indicative of a spatially constant CO/N_2 ice mixing ratio. In addition, even if pure CO patches occurred on Triton's surface, they would probably not be able to elevate the CO atmospheric abundance by means of the mechanism envisaged for Pluto methane. This is because CO is not buoyant in N_2, restricting the dispersal of CO-rich gas in the background atmosphere and therefore the sublimation rates of the CO patches (Stansberry et al. 1996). The detailed balancing model instead provides a physically-expected interpretation of the atmospheric CO/N_2 mixing ratio being consistent with its value in the ice phase (Fig. 5). Based on this scenario, the N_2-CO composition of the surface boundary layer ("film") can
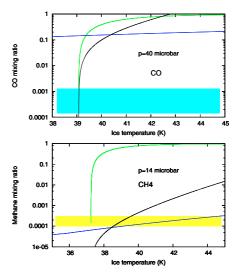

Fig. 6. Atmospheric mixing ratios and composition of the ice boundary layer ("film") in the detailed balancing model. (*Top*): CO-N_2 system. A surface pressure of 40 μbar is assumed, as estimated for 2009. The dark blue line is the CO/N_2 mixing ratio expected for pure ices. The green curve shows the CO mole fraction in the ice surface film, and the black curve is the CO/N_2 atmospheric mixing ratio derived from the composition of the ice film by applying Raoult's law. The range of CO/N_2 atmospheric mixing ratios inferred in this work for this pressure (($2-18$)$\times 10^{-4}$) is indicated by the blue-colored region. It implies a CO/N_2 mixing ratio in the surface film of $(1.4-12)\times 10^{-3}$ (see text). The surface film is therefore largely dominated by N_2, and the total pressure is defined by N_2 equilibrium at 39.075 K. (*Bottom*): CH_4-N_2 system. Calculations are here performed for a 14 μbar pressure, appropriate for the Voyager conditions. The Voyager-determined CH_4/N_2 atmospheric mixing ratio at the surface level (($1.1-3$) $\times 10^{-4}$) is indicated by the yellow region. The colored lines have the same meaning as in the top panel, with CH_4 replacing CO. The intersection of the black line with the colored area shows that explaining the observed CH_4 mixing ratio and the total pressure requires a 38.3–39.6 K surface temperature and would imply a very high CH_4 mole fraction (50–80%) in the surface film, well beyond the solubility limit of CH_4 in N_2. The same conclusion is reached if the CH_4 amounts measured in 2009 are used. Note that these diagrams remain similar at other surface pressures, the only change being the required ice temperature to sustain the total pressure.

be established by simple application of Raoult's law, providing $q_{CO}(\text{film}) = q_{CO}(\text{atm})\times p_{sat}(CO) / p_{sat}(N_2)$ (Trafton et al. 1998). Adopting again p = 40 μbar, our observed $q_{CO}(\text{atm})$ = ($2-18$) $\times 10^{-4}$ indicates $q_{CO}(\text{film})$ = $(1.4-12) \times 10^{-3}$. Therefore the surface veneer is still dominated by N_2 and the presence of CO does not significantly modify the N_2 atmospheric pressure, defined by equilibrium at 39.1 K (Fig. 6). Because it may be as thin as a few molecular layers, the surface film may not be visible in the near-IR spectra.

The case for CH_4 is more complex. As previously realized (Cruikshank et al. 1993; Yelle et al. 1997; Strobel & Summers 1997; Strobel et al. 1996), the CH_4 atmospheric mixing ratio at the surface measured by Voyager ($\sim 1.8 \times 10^{-4}$) is at least three orders of magnitude higher than expected for an ideal mixture. However, we note that it is also smaller, by a factor of ~6, than the ice CH_4/N_2 mixing ratio, and as such does not agree with the detailed balancing model in its simplest form. Unlike CO, CH_4 is subject to atmospheric photolysis and mass separation, and its vapor pressure is more temperature-dependent. This probably makes the surface/atmosphere abundance relationship for CH_4 complex and seasonally variable. In any case, the phase diagram of N_2-CH_4 is not obviously consistent with the formation of a CH_4-rich solid solution veneer (Stansberry et al. 1996).

Explaining the range of observed CH_4 atmospheric abundance would require a CH_4 mole fraction in the surface film as high as 50–80 % (Fig. 6), well beyond the solubility limit of CH_4 in N_2 (Prokhvatilov & Yantsevich 1983). The formation of pure CH_4 ice grains, decoupled from the mixture and not influencing its sublimation (Stansberry et al. 1996; Spencer et al.1997), further evolving into a lag deposit, may be a more plausible outcome. Using a Bond albedo of 0.85 (Triton's polar cap) and an emissivity of 0.7–1, a reasonable subsolar temperature for these pure methane patches is 45–48 K. Applying the Stansberry et al. (1996) Pluto model, we then find that methane patches covering 0.5–1% of Triton's surface are sufficient to maintain a $\sim 2 \times 10^{-4}$ atmospheric mixing ratio. Although there is no evidence of such patches in Triton's near-IR spectrum, the methane longitudinal distribution of CH_4 ice differs from that of N_2, and small areas of CH_4-dominated ice, notably near 300° longitude, are not inconsistent with observations (Grundy et al. 2010). In contrast, the existence of widespead pure methane ice is ruled out; therefore the emphasized fact that the Voyager-measured methane partial pressure was consistent with vapor pressure equilibrium of pure CH_4 ice at 38 K is probably coincidental.

After the Voyager encounter, a variety of seasonal N_2 cycle models (see review in Yelle et al. 1997) were explored in attempting to explain Triton's visual appearance and the then measured surface pressure. These models, which essentially differed in terms of the assumed ice and substrate albedos and thermal inertia, had limited success, leaving unanswered the simple question of where the ice is on Triton. Yet, they made distinctive predictions about the short-term evolution of Triton's atmosphere. High thermal inertia models predicted a pressure increase as Triton approached and passed Southern summer solstice in 2000 (Triton subsolar latitude moved from 45.5 S in 1989 to a maximum 50 S in 2000 and 47 S in 2009). This is a consequence of increased insolation on, and attendant sublimation of, the Southern polar cap (Spencer & Moore 1992; Forget et al. 2003). In contrast, "dark frost" models (Hansen & Paige 1992) or low thermal inertia models predicted a pressure decrease from $\sim$1980 onwards, due to the exhaustion of the seasonal southern cap and recondensation of N_2 on the invisible winter pole. The discovery of the pressure increase in the 1990's, and the persisting signature of N_2 and other ices in Triton reflectance spectrum with no obvious temporal evolution (Grundy et al. 2010), strongly argue that the bright deposits covering most of Triton southern hemisphere are relatively stable seasonal deposits. Our observation that the methane partial pressure has increased by a factor of $\sim$4 from 1989 to 2009 is qualitatively consistent with the reported pressure increase and the above interpretation. Since the CH_4 vapor pressure varies more sharply with temperature than N_2, we expect the atmospheric methane to be currently increasing more rapidly than pressure, but multi-volatile seasonal models will be needed to fully interpret our results. A direct measurement of Triton's current pressure is also highly desirable, and could be obtained by redetermining the N_2 ice temperature from its 2.15 μm band (Tryka et al. 1994).

The detection of CO also has implications for Triton's atmospheric thermal structure, photochemistry, and ionosphere. CO is an important cooling agent, by means of radiation in its rotational lines (Krasnopolsky et al. 1993; Strobel & Summmers 1997; Elliot et al. 2000b). It enriches atmospheric chemistry by introducing additional oxygen species (Krasnopolsky & Cruikshank 1995). Most importantly, it profoundly modifies

ionospheric composition by providing a source of C atoms and C^+ ions and by suppressing the N^+ concentration at the benefit of CO^+ and NO^+ (see review in Strobel & Summers 1997). Although the error bar on the CO abundance is large, all previous considerations on the role of CO now have direct observational support.

During the same observing night, we also searched for CO in Pluto's atmosphere, covering the region of the (3–0) band near 1.57 μm. Only an upper limit (1 cm-am) was obtained. For a characteristic surface pressure of 15 μbar (Lellouch et al. 2009), this indicates $CO/N_2 < 5 \times 10^{-3}$. While an improvement over previous results (Bockelée-Morvan et al. 2001; Young et al. 2001), this upper limit does not provide a strong constraint when compared to the measured CO ice mole fraction (1×10^{-3}, Douté et al. 1999). Nonetheless, given the similarity of the two bodies, the above considerations about surface control of atmospheric CO at Triton should also apply to Pluto. In 2015, observations with the ALICE and Rex instruments on New Horizons will provide measurements of the surface pressure and CH_4 and CO abundance in Pluto's atmosphere. We anticipate that CO will be measured at a uniform ratio of 0.001 and that the methane mixing ratio will show horizontal variability associated with local time and methane patch distribution.

References

Broadfoot, A. L., Atreya, S. K., Bertaux, J. L., et al. 1989, Science, 246, 1459
Bockelée-Morvan, D., Lellouch, E., Biver, N., et al. 2001, A&A, 377, 343
Cruikshank, D. P., Roush, T. L., Owen, T. C., et al. 1993, Science, 261, 742
Douté, S., Schmitt, B., Quirico, E., et al. 1999, Icarus, 142, 421
Elliot, J. L., Hammel, H. B., Wasserman, L. H., et al. 1998, Nature, 393, 765
Elliot, J. L., Person, M. J., McDonald, S. W., et al. 2000a, Icarus, 148, 347
Elliot, J. L., Strobel, D. F., Zhu, X., et al. 2000b, Icarus, 143, 425
Forget, F., et al. 2000, BAAS, 32, 45.01
Fray, N., & Schmitt, B. 2010, Planet. Space. Sci., in press
Grundy, W. M., Young, L. A., Stansberry, J. A., et al. 2010, Icarus, 205, 594
Gurrola, E. M. 1995, Ph.D. Thesis, Stanford University, Palo Alto
Hansen, C. A., & Paige, D. A. 1992, Icarus, 99, 273
Herbert, F., & Sandel, B. R. 1991, JGR, 96, 19241
Kaeufl, H.-U., Ballester, P., Biereichel, P., et al. 2004, SPIE, 5492, 1218
Krasnopolsky, V. A., & Cruikshank, D. P. 1995, JGR, 100, 21271
Krasnopolsky, V. A., Sandel, B. R., Herbert, F., et al., R.J. 1993, JGR, 98, 3065
Lellouch, E., Sicardy, B., de Bergh, C., et al. 2009, A&A, 495, L17
Olkin, C. B., Elliot, J. L., Hammel, H. B., et al. 1997, Icarus, 129, 178
Prokhvatilov, A. I., & Yantsevich, L. D. 1983, Sov. J. Low Temp. Phys. 9, 94
Quirico, E., Doute, S., Schmitt, B., et al. 1999, Icarus, 139, 159
Sicardy, B., et al. 1998, BAAS, 30, 49.02
Spencer, J. R., & Moore, J. M. 1992, Icarus, 99, 261
Spencer, J. R., et al. 1997, in Pluto and Charon, ed. S. A. Stern, & D. J. Tholen (The University of Arizona Press), 435
Stansberry, J. A., Spencer, J. R., Schmitt, B., et al. 1996, Planet. Space Sci. 44, 1051
Strobel, D. F., & Summers, M. E. 1995, in Neptune and Triton, ed. D.P. Cruikshank (The University of Arizona Press), 1107
Strobel, D. F., Zhu, X., & Summers, M. E. 1996, Icarus, 120, 266
Trafton, L. M. 1990, ApJ, 359, 512
Trafton, L. M., Matson, D. L., & Stansberry, J. A. 1998, in Solar System Ices, ed. B. Schmitt, C. de Bergh, & M. Festou (Kluwer Academic Publishers), 773
Tryka, K. A., Brown, R. H., Chruikshank, D. P., et al. 1994, Icarus, 112, 513
Yelle, R. V., Lunine, J. I., Pollack, J. B., et al. 1995, in Neptune and Triton, ed. D.P. Cruikshank (The University of Arizona Press), 1031
Young, L. A., Elliot, J. L., Tokunaga, A., et al. 1997, Icarus, 127, 258
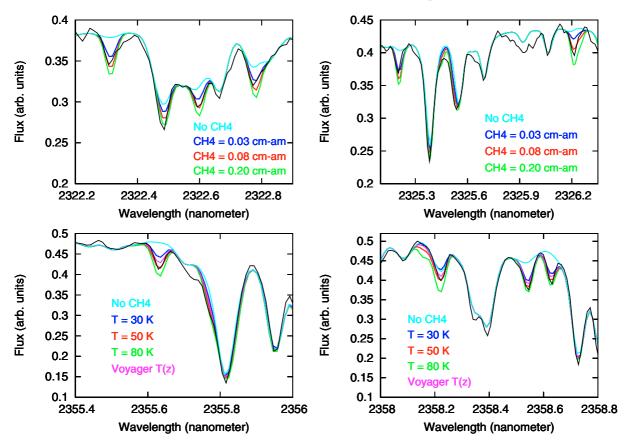Young, L. A., Cook, J. C., Yelle, R. V., et al. 2001, Icarus, 153, 148

Fig. 2. Zoomed image of several CH$_4$ lines showing sensitivity of the spectrum to Triton's methane. Some portions of the spectrum, especially over 2320–2326 nm, are relatively independent of temperature, while high–energy lines at 2353–2359 nm show increased temperature sensitivity. The *top two panels* show sensitivity to the methane abundance. Blue, red, and green synthetic spectra have 0.03, 0.08, and 0.20 cm-am of methane. Triton's thermal profile is taken from Krasnopolsky (1993) and a Voyager-like vertical distribution is used for methane (Herbert & Sandel 1991, entrance profile). Based on these models, the best fit methane column density is determined to be 0.08 ± 0.03 cm-am (i.e. ±40%). The bottom two panels show sensitivity to methane temperature. The previous best-fit model using Voyager thermal profile is shown in pink. Other models assume an isothermal atmosphere with temperature of 30 K (dark blue), 50 K (red) and 80 K (green). These fits indicate a mean methane temperature of 50^{+20}_{-15} K.
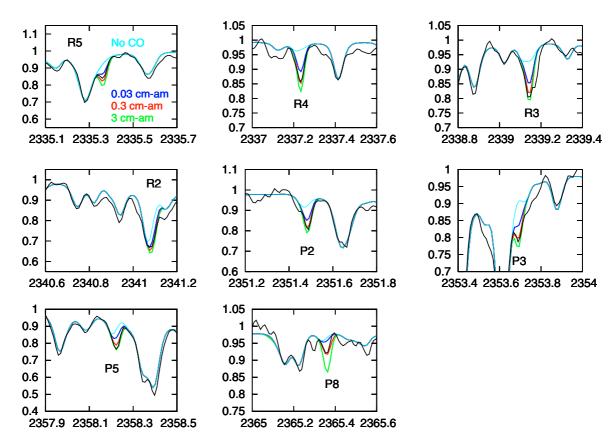
Fig. 4. The eight detected CO lines from Triton's atmosphere. *X*-axis units are nm and *Y*-axis units are arbitrary. Lines are compared with models including 0, 0.03, 0.30, and 3 cm–am of CO. The slow change in absorption depth with change of column density is caused by heavy saturation of particularly narrow Doppler–shaped lines at $T \sim 50$ K. Based on these models, the best fit CO column density is determined to be 0.30 cm-am with a factor of 3 uncertainty.